ORIGINAL ARTICLE

# Assessment of ultrasound-assisted forward osmosis process performance for seawater desalination using experimental factorial design

**Bara A. K. Al-Sakaji[1] · Sameer Al-Asheh[2] · Munjed A. Maraqa[1,3]**

© The Author(s) 2022

## Abstract

The effect of ultrasound on water flux through forward osmosis membrane for seawater desalination was investigated using the factorial design approach. Sodium chloride (NaCl) was used to simulate the dissolved solids content. In every test, the initial draw solution (DS) concentration was fixed at 4.5 M for NaCl and 2 M for $MgCl_2$. Parameters considered in the investigation included membrane crossflow velocity (0.25 and 1.0 cm/s), flow configuration (co-current versus counter-current), direction of ultrasound waves relative to the membrane side (active layer versus support layer), and type of draw solution (NaCl versus $MgCl_2$). A two-level factorial design was considered in the analysis of the results obtained from the experimental work. Based on the factorial design analysis, crossflow velocity and use of ultrasound have a positive effect on water flux enhancement for both draw solutions. However, the velocity effect on water flux enhancement was more pronounced than that of the use of ultrasound. The effect of flow configuration was statistically insignificant for both draw solutions. The interaction effect between crossflow velocity and ultrasound was statistically significant for both draw solutions. However, the interaction between crossflow velocity and flow configuration was only significant for the case of $MgCl_2$. The three-way interaction was insignificant for both draw solutions. The developed factorial model equations were used to predict other flux data in ultrasound-assisted FO systems and showed adequate representation of these data at relatively similar conditions after adjustment of the model for the baseline conditions of the evaluated cases.

**Keywords** Forward osmosis · Ultrasound · Water flux · Concentration polarization · Fouling · Scaling · Seawater · Factorial design

## Introduction

Forward osmosis (FO) is considered an emerging technology for water desalination. It can desalinate seawater with less energy and at potentially lower costs than reverse osmosis (RO). The process, just like RO, requires a selectively permeable membrane separating two fluids with different osmotic pressures and was first observed by Albert Nollet in 1748 (Nollet 1764). While in RO water is forced through the membrane using hydraulic pressure to overcome the natural osmotic pressure, FO, on the other hand, uses natural osmotic pressure to induce the flow of water through the semipermeable membrane by running a highly saline draw solution on the other side of the membrane. Thus, freshwater passes through the semipermeable membrane from the low to the high concentration solution due to the osmotic pressure gradient. This means that water in the feed solution flows through the membrane at a relatively low pressure which eliminates the need for high-pressure hydraulics in RO specially when dealing with high saline water. This constitutes the main difference between FO and RO. The main advantages of the FO process include its low power consumption, easy to scale up, and potential high recovery

✉ Sameer Al-Asheh
   sslasheh@aus.edu

✉ Munjed A. Maraqa
   m.maraqa@uaeu.ac.ae

[1] Department of Civil and Environmental Engineering, College of Engineering, United Arab Emirates University, P.O. Box 15551, Al-Ain, United Arab Emirates

[2] Department of Chemical Engineering, College of Engineering, American University of Sharjah, P.O. Box 2666, Sharjah, United Arab Emirates

[3] National Water and Energy Center, United Arab Emirates University, P.O. Box 1551, Al-Ain, United Arab Emirates

rate (Robert and Menachem 2007; Kah et al. 2011; Tzahi et al. 2006). The operating cost of FO process is much lower than RO and thermal processes. Different chemical compounds have been used as a draw solution in FO process such as table salt, magnesium sulfate, glucose, ammonia carbon dioxide, and magnesium chloride (Tai-Shung et al. 2012). In practice, the draw solution is recycled and reused to reduce the cost of desalination. This is typically achieved either by thermal or membrane filtration processes.

Due to several operational issues, the FO has only been implemented to a limited extent, which restricts its proper use in large-scale commercial applications. These challenges include fouling, internal/external concentration polarization (CP), solute diffusion from the draw solution to the feed solution or vice versa, and regeneration/separation of the draw solution (Qasim et al. 2017; Xu et al. 2010). These restrictions reduce the system's water flux and recovery rate, which has a detrimental influence on system performance and eventually raises the cost of water purification. While membrane fouling and concentration polarization cannot be ignored in the FO process and must be mitigated or controlled to improve process efficiency (Lee et al. 2020), the FO process is anticipated to typically have a lower surface fouling tendency than the RO (Qasim et al. 2015). Numerous methods for reducing and controlling FO membrane fouling/CP and improving process efficiency have been documented in seawater desalination. These include conventional and unconventional pre-treatment techniques, chemical dosing, membrane surface changes, system operating condition optimization, and appropriate draw solution selection (Qasim et al. 2015).

In water and wastewater membrane treatment and desalination applications, the use of ultrasound has recently been proposed as a pretreatment system or a membrane cleaning technique that would improve membrane systems performance. It should be highlighted that the use of ultrasound requires cautious consideration because doing so at specific frequencies and configurations could harm the membranes (Qasim et al. 2018). The use of ultrasound for membrane cleaning and flux enhancement has been recently considered in the FO osmosis process but received less attention and requires more investigation to be conducted for process enhancement. Studies on coupling ultrasound with FO have been recently reviewed by Al-Sakaji et al. (2022a). The review addressed questions related to implementation of an ultrasound/FO system for seawater desalination, such as the impact on fouling, flow configuration, and location of fouling. The authors also discussed the mechanisms for the impact of ultrasound on FO membranes. In another study, Al-Sakaji et al. (2022b) investigated the effect of using ultrasound on water flux through a forward osmosis membrane when applied to seawater desalination (Al-Sakaji et al. 2022b). Using scaling

agents and organic foulants, a synthetic solution was deployed by the authors to simulate seawater. They concluded that applying a continuous ultrasound frequency of 40 kHz was effective in enhancing water flux, especially when the ultrasound source faces the membrane active layer, irrespective of the used draw solution. They also observed that the use of ultrasound generally caused an adverse effect on the water flux when the ultrasound source faces the membrane support layer. In general, they found that higher water flux enhancement was achieved with NaCl as a draw solution compared to that of $MgCl_2$ when used as a draw solution.

The previous work by Al-Sakaji et al. (2022b) considered the effect of several operating parameters on the water flux of the FO membrane for seawater desalination applications. Investigated parameters included membrane cross-flow velocity, flow configuration (co-current vs. counter-current), direction of ultrasound waves relative to the membrane faces (active layer vs. support layer), and types of the draw solution (NaCl versus $MgCl_2$) (Al-Sakaji et al. 2022b). In this paper, a two-level factorial design ($2^k$) is used to analyze the results obtained from the experimental data. This facilitates studying the effect of each of the selected parameters ($k$) and their interactions on the membrane water flux performance (the response variable) and identifies the most influential parameters on the process performance accordingly.

## Materials and methods

### Materials

In order to simulate the salinity, scaling agents, and algae features of seawater as closely as possible, the feed solution (FS) was created utilizing a variety of ingredients. Calcium sulfate dihydrate ($CaSO_4 \cdot 2H_2O$) was used to represent inorganic fouling and scaling materials (Choi et al. 2013; Kim et al. 2012), sodium alginate was used to simulate the algal organic matter biofouling that would exist in seawater intakes (Mi and Elimelech 2008), and sodium chloride (NaCl) was used to simulate the dissolved solids content (Qasim et al. 2020). In every test, the initial draw solution (DS) concentration was fixed at 4.5 M for NaCl and 2 M for $MgCl_2$. The suggested concentrations produced values of almost equal osmotic pressure (Cath et al. 2006). FTSH2O™ flat sheet cellulose triacetate (CTA) embedded support FO membranes were used in this work. The membranes were manufactured by Fluid Technology Solution, Inc. (Albany, USA) and procured from Sterlitech (Kent, USA) Additional information regarding the materials and chemicals used is provided elsewhere (Al-Sakaji et al. 2022b).

## Experimental work

The performance of the FO membrane (water flux) in presence of ultrasound for seawater desalination was examined in this paper using three operating parameters. These include the crossflow velocities at both membrane sides, the flow configuration set up, and the membrane orientation with respect to the ultrasonic source. NaCl and $MgCl_2$ were the two types of draw solutions for which these parameters were examined. A fixed feed and draw solutions crossflow velocity (CFV) and two velocity levels were selected. Two flow configuration arrangements, co-current (FS and DS flow in the same direction), and counter-current (FS flow in the opposite direction of the DS flow) were considered. The exposure of the membrane surface to ultrasound was also tested (i.e., the active layer faces the transducer or when the support layer faces the transducer). Two draw solutions of NaCl and $MgCl_2.6H_2O$ were tested. A summary of the experimental tests that were conducted is given in Table 1. In this table, Factor 1 refers to the case where the CFV was at 0.25 and 1.0 cm/s, Factor 2 refers to the flow configuration of co-current (C) and counter-current (CC) flow, and Factor 3 refers to transducer location which was either at the active layer (AL) or the support layer (SL) side. For each run, a baseline experiment (control) was conducted at the beginning of the test, at the full-intended experimental conditions without having the ultrasound bath on board. In this work, all tests were conducted using the FO mode (AL-FS). It should be mentioned that the tests were randomized to reduce the impact of outside influences on the results. Additionally, all configurations that were evaluated were duplicates, and average values shall be presented.

## Experimental setup and procedure

For each test, a brand-new membrane was used. The membrane sheet was cut to fit the size of the testing cell in accordance with the manufacturer's instructions before being rinsed with DI water to get rid of the membrane preservative solution. The testing cell has two channels separated by the FO membrane. Each channel is 81 mm long, 60 mm wide, and 24 mm deep, providing a membrane surface area of around 48.6 $cm^2$. More details about the experimental setup are provided elsewhere (Al-Sakaji et al. 2022b).

All tests in this study were conducted in an AL-FS FO mode where the FS was introduced, tangentially, to the membrane active layer (smooth surface) while the DS at the side of the membrane support layer (rough surface). Depending on the required flow configuration (C or CC), appropriate piping system was connected to the testing cell ports. The simulated seawater FS was provided to the unit using a diaphragm pump (Model TYP-9600-kJ, Deng Yuan Industrial Co., Ltd, Taiwan), in a closed-loop storage graduated cylinder (1 L capacity). The FS storage was placed on the top of a digital balance to measure the change in FS weight over time. The same way was made for the DS recirculation pumping, where the DS was pumped tangentially to the membrane support layer at a CFV equals to the FS flow velocity and return to the DS storage graduated cylinder (1 L capacity) by another pump similar to the one used for FS pumping. The required CFV (= flow rate/cell

**Table 1** Testing arrangement for NaCl and $MgCl_2$ draw solutions with ultrasound irradiation

| Test No. | NaCl DS Run No. | MgCl$_2$ DS Run No. | CFV (cm/s) (Factor 1) | Flow configuration (Factor 2) | Transducer location (Factor 3) |
|---|---|---|---|---|---|
| 1 | 10 | 10 | 0.25 | C | AL |
| 2 | 8 | 14 | 1.0 | C | AL |
| 3 | 16 | 12 | 0.25 | CC | AL |
| 4 | 14 | 8 | 1.0 | CC | AL |
| 5 | 2 | 13 | 0.25 | C | SL |
| 6 | 7 | 9 | 1.0 | C | SL |
| 7 | 1 | 6 | 0.25 | CC | SL |
| 8 | 6 | 4 | 1.0 | CC | SL |
| 9 | 11 | 11 | 0.25 | C | AL |
| 10 | 12 | 2 | 1.0 | C | AL |
| 11 | 13 | 5 | 0.25 | CC | AL |
| 12 | 15 | 16 | 1.0 | CC | AL |
| 13 | 9 | 3 | 0.25 | C | SL |
| 14 | 5 | 7 | 1.0 | C | SL |
| 15 | 3 | 1 | 0.25 | CC | SL |
| 16 | 4 | 15 | 1.0 | CC | SL |

cross-sectional area) was obtained by changing the pump flow rate. For example, to obtain CFV of 0.25 and 1.0 cm/s, the pump flow rate was fixed at around 0.3 L/min and 1.1 L/min, respectively. When the system was completely assembled, air bubbles inside the system were released by pumping the FS and DS for a short time. For all tests, the initial volumes of the FS and DS were both kept equal at around 670 mL. This value was mainly selected in order to have a buffer volume in the DS cylinder so as to accommodate the water molecules transferred from the FS toward the DS cylinder.

A continuous ultrasound wave with a fixed frequency of 40 kHz was used to investigate how ultrasound affects membrane flux. The FO testing cell was placed in an ultrasonic bath (Model No. 3510 DTH Ultrasonic Cleaner, Branson Ultrasonics, CT, USA) filled with potable water and located 20 mm from the bottom of the tank. The ultrasonic bath has a length of 29.2 cm, a width of 15.2 cm, and a depth of 15.2 cm. The device was fitted with two built-in transducers fixed at the bottom of the tank. The device provides an output power of 37.9 W (Qasim et al. 2020), which results in an ultrasound intensity on the membrane surface of about 0.09 W/cm$^2$. Figure 1 depicts the experimental setup for one of the investigated configurations, AL-FS mode, co-current, and active layer (AL) facing ultrasound transducer. Further details about the experimental setup, procedure followed, and instruments used for measurements of temperature, pH, and conductivity are described elsewhere (Al-Sakaji et al. 2022b).

The water flux through the membrane is used to determine the FO process performance. Equation (1) was used to compute the water flux through the membrane based on measuring the change in the mass of the FS throughout the relevant experiment test (Qasim et al. 2020).

$$J_w = \frac{\Delta m}{\rho_w S \Delta t} \tag{1}$$

where, $J_w$ is the calculated water flux (L/m$^2$·h), $\Delta m$ is the change in the mass of the FS (g), $\rho_w$ is the water density (assumed to be 1000 g/L), $S$ is the membrane effective surface area (0.00486 m$^2$), and $\Delta t$ is the duration that corresponds to $\Delta m$ (h).

The calculation was carried out independently for each of the two draw solutions that were chosen as well as for the baseline situation without the ultrasonography. The average flux value for the replicate experiments was considered. Values of the average flux under baseline

Table 2 Average flux (L/m$^2$·h) under baseline conditions for NaCl and MgCl$_2$ DSs

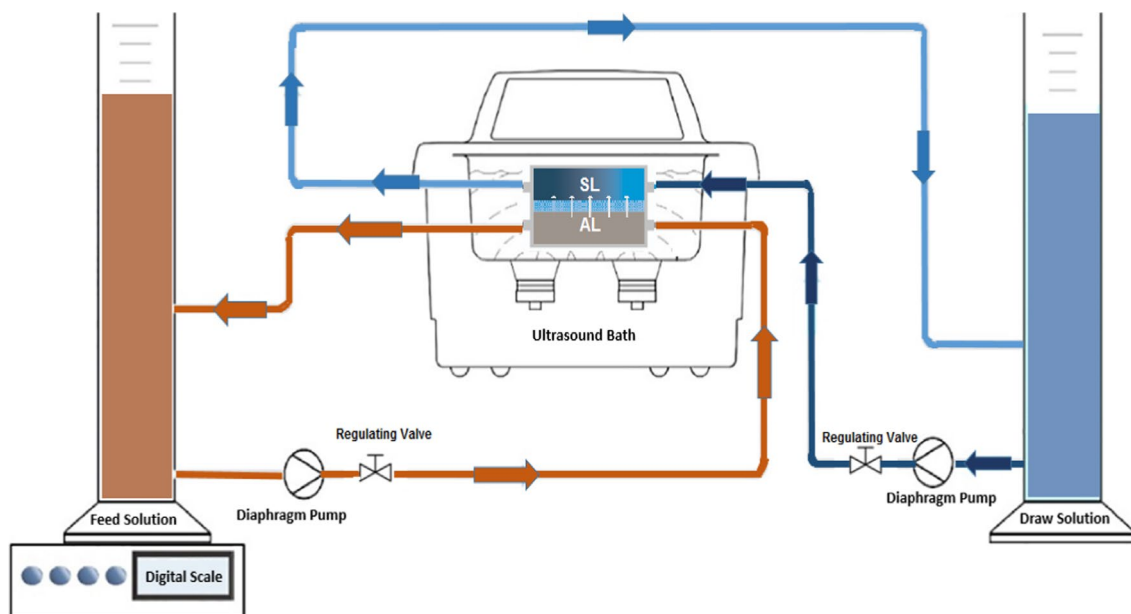| CFV (cm/s) | Flow Configuration | Flux for NaCl DS | Flux for MgCl$_2$ DS |
|---|---|---|---|
| 0.25 | C | 7.95 | 4.33 |
| 1.0 | C | 14.44 | 10.32 |
| 0.25 | CC | 6.57 | 5.08 |
| 1.0 | CC | 12.51 | 9.71 |



**Fig. 1** Experimental setup arrangement for ultrasound-assisted FO process: AL-FS mode, co-current and the active layer (AL) faces the ultrasound transducer (Al-Sakaji et al. 2022b)

conditions for the used draw solutions are presented in Table 2.

## Statistical analysis/regression model

The effect of each of the selected parameters and their interactions on the membrane water flux performance (the response variable) have been statistically estimated. As such, the following items were covered in this work for the analysis of the collected data by utilizing the Minitab software:

1. Calculate the main effects of all selected factors and their interactions,
2. Construct the analysis of variance (ANOVA) tables, and
3. Generate the relevant regression models.

## Factorial design

The effect of the operating parameters is normally studied based on the effect of one factor or input at a time on the response variable or the output. However, this method does not consider the effect of the interaction between different factors that could also have an impact on the response variable (Mason et al. 2003). However, the factorial design method is used to better understand the system behavior, taking into account the effect of the different system input parameters individually as well as their interactions that ultimately contribute to the response variable (Montgomery 2013).

Factorial design provides flexibility that allows studying response behavior of one factor at different levels of other factors within the same run (Seltman 2018). The effect of any factor can be defined as the change in the average response generated by the average change in the level of that factor. This is typically known as the main effect (Montgomery 2013). Table 3 illustrates the factorial design matrix for $2^3$ designs, i.e., requiring 8 experimental runs.

Linear regression models are considered as one of the most commonly used statistical approaches that helps in predicting the value of the dependent variable (response) based

on the value of other involved independent variables (factors) (Seltman 2018). In this work, a regression model for the $2^3$ factorial design experiment was developed to estimate and explain the relationship between quantitative variables and/or qualitative variables and their interactions. The use of the regression model allows predicting the value of the output response based on the value of other independent variables (factors). The general regression model for a $2^3$ factorial design model can be written as:

$$Y = \beta_0 + \beta_1 X_1 + \beta_2 X_2 + \beta_3 X_3 + \beta_{12} X_1 X_2 \\ + \beta_{13} X_1 X_3 + \beta_{23} X_2 X_3 + \beta_{123} X_1 X_2 X_3 + \varepsilon \tag{2}$$

where $Y$ is the dependent variable (response), $X_1$, $X_2$ and $X_3$ are the assigned independent variables for velocity, flow configuration, and ultrasound orientation, respectively, the different $\beta$s correspond to the regression model coefficients, and $\varepsilon$ is the experimental error.

Based on the above and as described earlier, the required statistical analysis in this work and its associated output figures are produced utilizing Minitab® 20 software (Minitab 2021) as will be shown in the following section.

## Results and discussion

### Full factorial design for NaCl DS

In this work, eight different configurations (2 replicates each at randomized manner) were conducted for each type of the used draw solutions (NaCl and $MgCl_2$). Thus, two separate $2^3$ full factorial design studies were conducted. As explained earlier, three parameters were selected to study their effects on the response variable (water flux). These include the CFV (Velocity), flow configurations (Flow Conf.), and the ultrasound source orientation toward the membrane surface (US Orien.), with each tested at two levels ($-1$ and $+1$). The $-1$ and $+1$ levels are, respectively, defined as 0.25 and 1.0 cm/s for the CFV, C and CC for the flow configuration, and AL and SL for the ultrasound orientation toward the membrane surface. The Minitab input matrix for the two replicates of the randomized $2^3$ full factorial design for the NaCl DS is shown in Table 4.

The Minitab outputs of the calculated average effects of the selected parameters and their interactions on the response variable (flux) are shown in Table 5.

According to the $p$ values (Table 5), there is a significant positive effect on the water flux ($p < 0.05$) of CFV (Velocity term) when changed from low (0.25 cm/s) to high (1.0 cm/s) values, and a significant positive effect of ultrasound orientation (US Orien. term) when changed from high (SL) to low (AL). Furthermore, the interaction between velocity and ultrasound orientation ($\beta_{13}$) has a

**Table 3** Design matrix for $2^3$ factorial designs

| Run | Factor 1 | Factor 2 | Factor 3 |
|-----|----------|----------|----------|
| 1 | $-1$ | $-1$ | $-1$ |
| 2 | $+1$ | $-1$ | $-1$ |
| 3 | $-1$ | $+1$ | $-1$ |
| 4 | $+1$ | $+1$ | $-1$ |
| 5 | $-1$ | $-1$ | $+1$ |
| 6 | $+1$ | $-1$ | $+1$ |
| 7 | $-1$ | $+1$ | $+1$ |
| 8 | $+1$ | $+1$ | $+1$ |

**Table 4** Minitab input matrix for $2^3$ full factorial design with 2 replicates for the NaCl DS

| Std Order | Run order | Center Pt | Blocks | Velocity | Flow Conf. | US Orien. | Flux (L/m²·h) |
|---|---|---|---|---|---|---|---|
| 1 | 10 | 1 | 1 | −1 | C | AL | 10.01 |
| 2 | 8 | 1 | 1 | 1 | C | AL | 14.64 |
| 3 | 16 | 1 | 1 | −1 | CC | AL | 11.23 |
| 4 | 14 | 1 | 1 | 1 | CC | AL | 15.01 |
| 5 | 2 | 1 | 1 | −1 | C | SL | 5.69 |
| 6 | 7 | 1 | 1 | 1 | C | SL | 12.83 |
| 7 | 1 | 1 | 1 | −1 | CC | SL | 4.85 |
| 8 | 6 | 1 | 1 | 1 | CC | SL | 13.9 |
| 9 | 11 | 1 | 1 | −1 | C | AL | 11.31 |
| 10 | 12 | 1 | 1 | 1 | C | AL | 15.32 |
| 11 | 13 | 1 | 1 | −1 | CC | AL | 11.21 |
| 12 | 15 | 1 | 1 | 1 | CC | AL | 15.32 |
| 13 | 9 | 1 | 1 | −1 | C | SL | 4.32 |
| 14 | 5 | 1 | 1 | 1 | C | SL | 13.58 |
| 15 | 3 | 1 | 1 | −1 | CC | SL | 6.4 |
| 16 | 4 | 1 | 1 | 1 | CC | SL | 13.55 |

**Table 5** Minitab output for the model coded coefficients for NaCl DS

| Term | Effect | Coef. | SE Coef. | T-value | p value | VIF |
|---|---|---|---|---|---|---|
| Constant, $\beta_0$ | | 11.198 | 0.168 | 66.71 | 0.000 | |
| Velocity, $\beta_1$ | 6.141 | 3.071 | 0.168 | 18.29 | 0.000 | 1 |
| Flow Conf., $\beta_2$ | 0.471 | 0.236 | 0.168 | 1.4 | 0.198 | 1 |
| US Orien., $\beta_3$ | −3.616 | −1.808 | 0.168 | −10.77 | 0.000 | 1 |
| Velocity × Flow Conf., $\beta_{12}$ | −0.119 | −0.059 | 0.168 | −0.35 | 0.733 | 1 |
| Velocity × US Orien., $\beta_{13}$ | 2.009 | 1.004 | 0.168 | 5.98 | 0.000 | 1 |
| Flow Conf. × US Orien., $\beta_{23}$ | 0.099 | 0.049 | 0.168 | 0.29 | 0.776 | 1 |
| Velocity × Flow Conf. × US Orien., $\beta_{123}$ | 0.069 | 0.034 | 0.168 | 0.2 | 0.843 | 1 |

significant positive effect on the water flux. The results also suggest an insignificant (weak) effect of flow configuration ($\beta_2$), and the 2-way interaction between velocity and flow configuration ($\beta_{12}$), and between flow configuration and ultrasound orientation ($\beta_{23}$). Similarly, there is an insignificant effect of the 3-parameter interaction between velocity, flow configuration, and ultrasound orientation ($\beta_{123}$).

Figure 2 shows plots of the main effects for the three selected parameters on the mean of water flux. According to these plots, increasing the flow velocity from the low (0.25 cm/s) to the high level (1.0 cm/s) significantly increases water flux. However, changing the flow configuration from a low level (C) to a high level (CC) causes a slight increase in water flux, but it is statistically insignificant based on the predefined significance level of 0.05. The insignificant effect of flow configuration could be attributed to the small dimensions of the testing cell, where the effect of changing the flow configuration does not appear to be clearly noticeable along the selected membrane dimensions. Phuntsho et al. (2013) also found no significant effect on the

water flux due to the change in the flow configuration and attributed this to the small size of the used testing cell.

Changing the ultrasound orientation from the high level (SL) to the low level (AL) causes a significant increase in water flux. Given that the feed solution has fouling and scaling materials, the active layer of the FO membrane is exposed to fouling problems that would cause flux reduction due to cake/gel layer formation (external fouling). Thus, the increase in water flux is attributed to the effect of using the ultrasound at the membrane active layer side. This agrees with the findings of Heikkinen et al. (2017), who reported flux enhancement upon applying ultrasound on the active layer of a CTA membrane. Meanwhile, it has been reported that the use of ultrasound minimizes the effect external concentration polarization by reducing solute concentration at the membrane boundary layer, reducing the external fouling effect by breaking the fouling (sulfate crystals and alginate gel) layer formed (Choi et al. 2014), and detaching the deposited substances on the membrane active layer (Aktij et al. 2020). This significantly reduces the system resistance and increases the membrane performance.
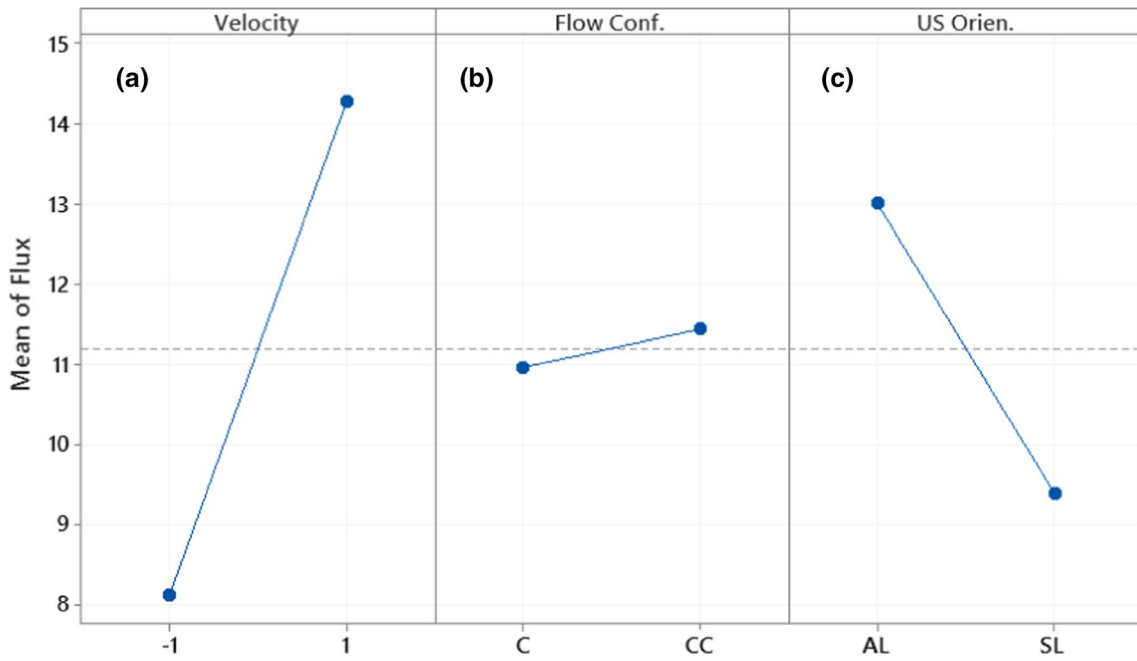
**Fig. 2** Plots of the main effects of **a** CFV, **b** flow configuration, and **c** ultrasound orientation on the water flux (L/m$^2$·h) for NaCl DS

Figure 3 shows the plots for the interaction effect between the different parameters on the water flux. According to these plots, the interaction between velocity and ultrasound orientation has a significant effect on the water flux. The figure reveals no significant interaction between velocity and flow configuration and between flow configuration and ultrasound orientation. This indicates the importance of CFV and ultrasound orientation and
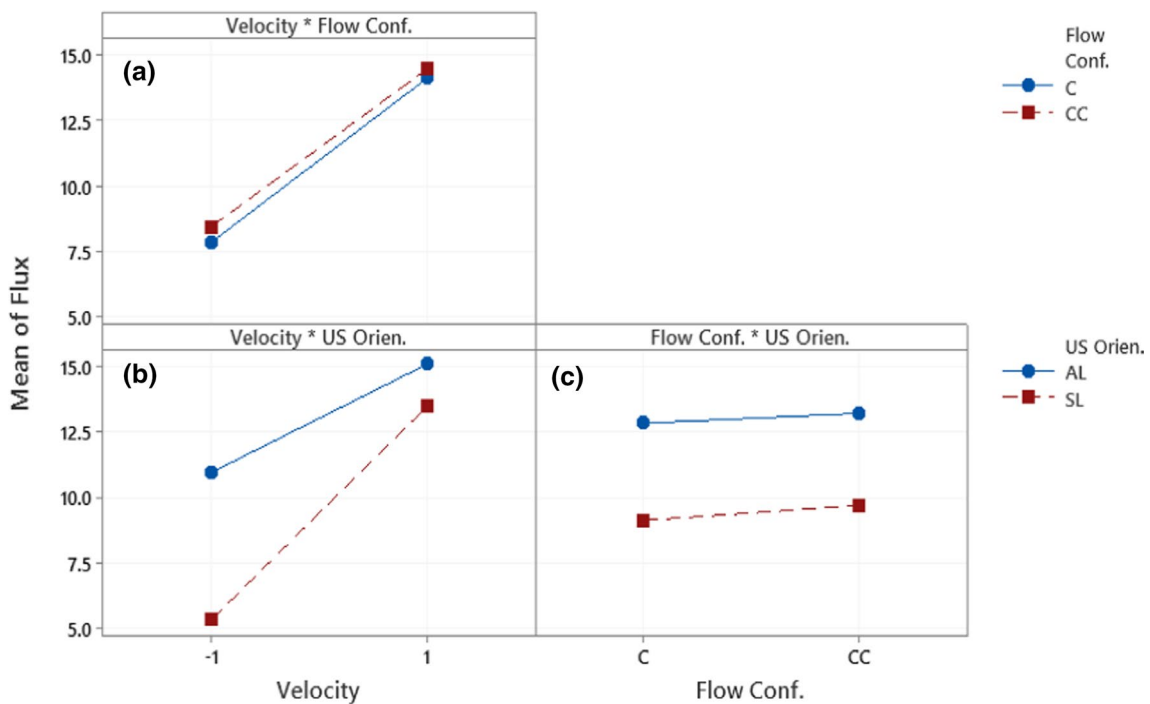


**Fig. 3** Plots of the interaction effects of **a** CFV with flow configuration, **b** CFV with ultrasound orientation, and **c** flow configuration with ultrasound orientation on the water flux (L/m$^2$·h) for NaCl DS

their interactions on the FO membrane flux enhancement when NaCl is used as a DS.

Minitab was used to develop the water flux regression model. The developed model is presented by Eq. (3):

$$
\begin{aligned}
Y = {}& 11.198 + 3.071X_1 + 0.236X_2 - 1.808X_3 \\
& - 0.059X_1X_2 + 1.004X_1X_3 + 0.049X_2X_3 \\
& + 0.034X_1X_2X_3
\end{aligned}
\tag{3}
$$

Figure 4 shows the generated residual plots for water flux using Minitab. The plots show that the data follow the normal probability, since the observed data approximately follow a straight line. This supports the assumption that the residuals (error) are normally distributed. Moreover, the calculated $p$ value from Ryan–Joiner (similar to Shapiro–Wilk) test provides a $p$ value of 0.077 which is greater than 0.05, confirming the validity of the normality assumption. Moreover, the Kolmogorov–Smirnov normality test was conducted through which the $p$ value was found to be 0.129.

Based on the above, it can be concluded that increasing the CFV causes a significant impact on the water flux but changing the ultrasound orientation from the membrane support layer to the active layer side causes a moderate effect. Changing the flow configuration causes an insignificant effect (minor effect) on the water flux. The interaction effect between the CFV and the ultrasound orientation causes the least significant effect, but still significant, on water flux as compared to the individual effect of these two parameters.

## $2^3$ Full factorial design for MgCl$_2$ DS

Similar to the approach followed for NaCl DS, Tables 6 shows the input design matrix and Table 7 shows the output of the calculated average effects of the previously selected parameters and their interactions on the response variable (flux) using MgCl$_2$ as a DS.

The results shown in Table 7 suggest that (based on $p$ values < 0.05) there is a significant positive effect in water flux due to shifting from low to high-velocity level, and a moderate positive effect due to changing the ultrasound orientation from high (SL) to low (AL) level. The obtained results agree with what was found in the NaCl test which provides strong evidence about the importance of the effect of flow velocity and ultrasound orientation on the membrane's performance. Like what was found in the NaCl test, the flow configuration in the MgCl$_2$ is statistically insignificant. However, the interaction between the flow configuration and the flow velocity has a marginal negative effect on water flux, which was not the case with the NaCl DS. A marginal positive effect of the interaction between flow velocity and ultrasound orientation was also observed. This agrees with the NaCl results; however, the interaction effect in the NaCl test was found to be more significant (about 2.8 times higher) than the one
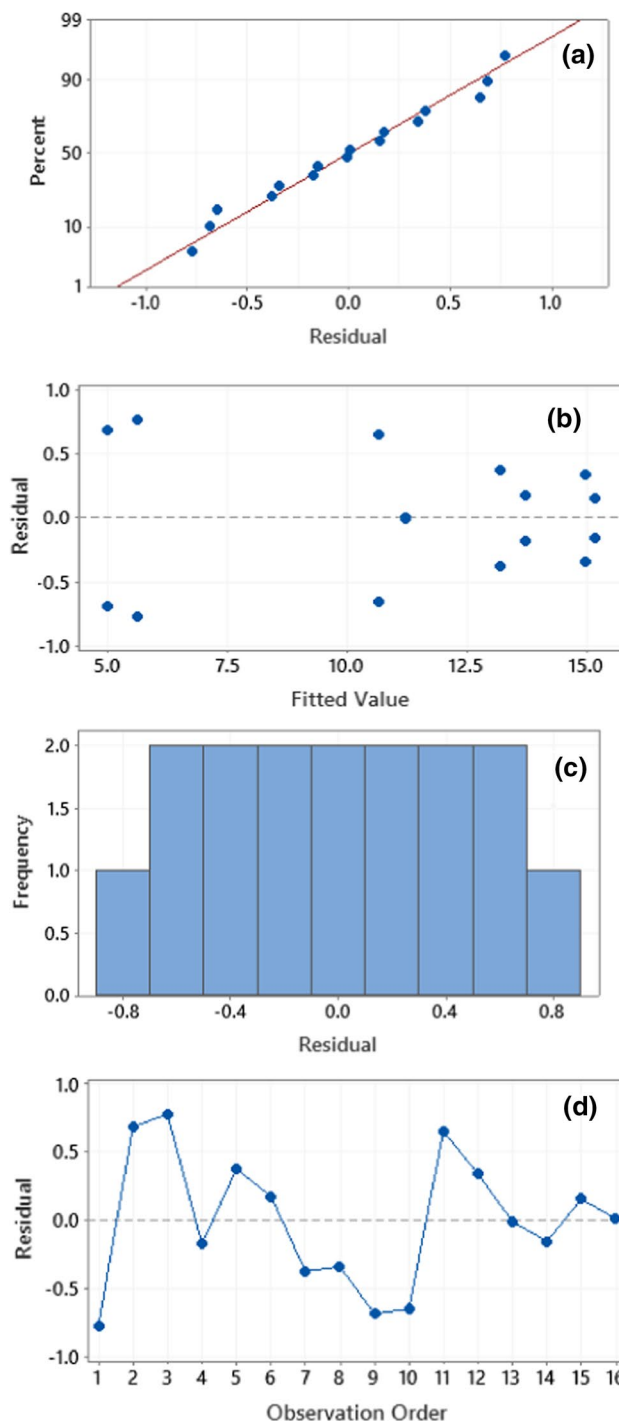


**Fig. 4** Residual plots for water flux (L/m$^2$·h) using NaCl DS showing **a** normal probability plot, **b** residual versus fitted flux value, **c** frequency versus residual, and **d** residual versus observation order

observed in the MgCl$_2$ test. Higher flux enhancement with NaCl draw solution compared to MgCl$_2$ draw solution could be mainly attributed to a higher diffusivity, lower viscosity, and lower molecular weight of NaCl (Cath et al. 2013). The smaller ion size of NaCl allows for better solute dispersion

**Table 6** Minitab input matrix for $2^3$ full factorial design with 2 replicates for MgCl$_2$ DS

| Std Order | Run order | Center Pt | Blocks | Velocity | Flow Conf. | US Orien. | Flux (L/m²·h) |
|---|---|---|---|---|---|---|---|
| 1 | 10 | 1 | 1 | −1 | C | AL | 6.64 |
| 2 | 14 | 1 | 1 | 1 | C | AL | 11.35 |
| 3 | 12 | 1 | 1 | −1 | CC | AL | 7.94 |
| 4 | 8 | 1 | 1 | 1 | CC | AL | 10.15 |
| 5 | 13 | 1 | 1 | −1 | C | SL | 4.95 |
| 6 | 9 | 1 | 1 | 1 | C | SL | 9.52 |
| 7 | 6 | 1 | 1 | −1 | CC | SL | 5.46 |
| 8 | 4 | 1 | 1 | 1 | CC | SL | 9.79 |
| 9 | 11 | 1 | 1 | −1 | C | AL | 7.40 |
| 10 | 2 | 1 | 1 | 1 | C | AL | 10.19 |
| 11 | 5 | 1 | 1 | −1 | CC | AL | 8.12 |
| 12 | 16 | 1 | 1 | 1 | CC | AL | 9.80 |
| 13 | 3 | 1 | 1 | −1 | C | SL | 4.34 |
| 14 | 7 | 1 | 1 | 1 | C | SL | 9.61 |
| 15 | 1 | 1 | 1 | −1 | CC | SL | 5.75 |
| 16 | 15 | 1 | 1 | 1 | CC | SL | 8.79 |

**Table 7** Minitab output for the model coded coefficients for MgCl$_2$ DS

| Term | Effect | Coef. | SE Coef. | T-value | p Value | VIF |
|---|---|---|---|---|---|---|
| Constant, $\beta_0$ | | 8.112 | 0.118 | 68.77 | 0.000 | |
| Velocity, $\beta_1$ | 3.577 | 1.789 | 0.118 | 15.16 | 0.000 | 1 |
| Flow Conf., $\beta_2$ | 0.226 | 0.113 | 0.118 | 0.96 | 0.365 | 1 |
| US Orien., $\beta_3$ | −1.67 | −0.835 | 0.118 | −7.08 | 0.000 | 1 |
| Velocity × Flow Conf., $\beta_{12}$ | −0.759 | −0.38 | 0.118 | −3.22 | 0.012 | 1 |
| Velocity × US Orien., $\beta_{13}$ | 0.727 | 0.363 | 0.118 | 3.08 | 0.015 | 1 |
| Flow Conf. × US Orien., $\beta_{23}$ | 0.12 | 0.06 | 0.118 | 0.51 | 0.626 | 1 |
| Velocity × Flow Conf. × US Orien., $\beta_{123}$ | 0.144 | 0.072 | 0.118 | 0.61 | 0.559 | 1 |

within the solution and thus provides a high diffusion rate that minimizes the system overall resistance and reduces the effect of internal concentration polarization which would enhance the water flux (Suwaileh et al. 2020). This is consistent with the findings of Achilli et al. (2010), who indicated that at the same osmotic pressure the flux produced by NaCl is higher than the one produced by MgCl$_2$.

The interaction between flow configuration and ultrasound orientation (Flow Conf. × US Orien.) and between velocity, flow configuration, and ultrasound orientation (Velocity × Flow Conf. × US Orien.) was not statistically significant, which is also consistent with what was observed with the NaCl DS.

The main effects of the crossflow velocity, flow configuration, and the ultrasound orientation on the mean value of flux are shown in Fig. 5. The trends shown (Fig. 5) for each parameter are like what was obtained in the NaCl DS (with a low value of the mean flux). The plots of Fig. 5 declare that the effect of increasing the flow velocity from the low level (−1) to the high level (+1) causes a large increase in the water flux, and that changing the flow configuration

from co-current to counter current causes a minor increase in water flux. The latter parameter is considered statistically insignificant as evidence of the associated $p$ value is less than the considered significance level of 0.05. Changing the ultrasound orientation from the high level (SL) to the low level (AL) causes a significant increase in water flux.

Figure 6 shows the effects of the interaction between the different parameters on the water flux. The interaction effect between the CFV and flow configuration is clearly reflected in the water flux (the co-current and counter-current lines are crossed). This interaction effect suggests that the relationship between the velocity and flow configuration depends on the value of the flow configuration. At the low-level velocity, the counter-current configuration is associated with the highest flux mean. However, at the high-velocity level, the co-current configuration provides higher flux than the co-current configuration. There is a moderate interaction between flow velocity and ultrasound orientation. Figure 6 shows that the highest flux is obtained in the case of the high-level velocity and the membrane active layer faces the ultrasound
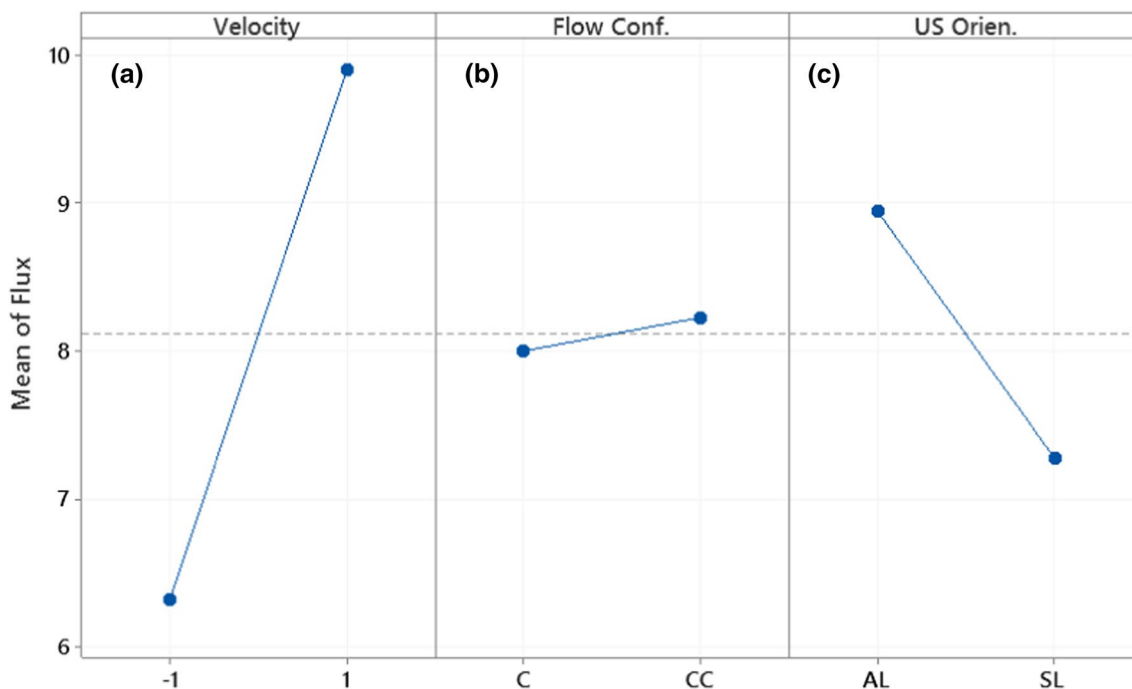
**Fig. 5** Plots of the main effects of **a** CFV, **b** flow configuration, and **c** ultrasound orientation on the water flux ($L/m^2 \cdot h$) for $MgCl_2$ DS
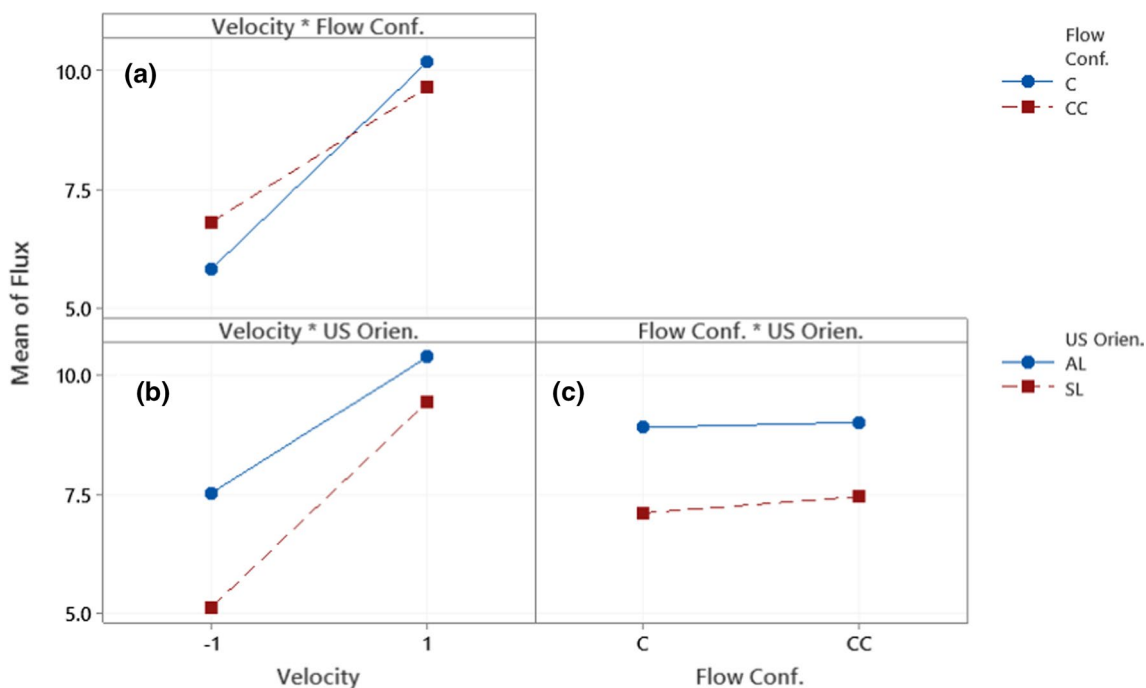


**Fig. 6** Plots of the interaction effects of **a** CFV with flow configuration, **b** CFV with ultrasound orientation, and **c** flow configuration with ultrasound orientation on the water flux ($L/m^2 \cdot h$) for $MgCl_2$ DS

transducer. Moreover, in the case of the membrane support layer facing the ultrasound transducer, a lower flux than the one obtained with the active layer facing the membrane was observed. Figure 6 also shows that the interaction

between flow configuration and ultrasound orientation is very weak and statistically insignificant. However, in the case of the membrane active layer facing the ultrasound source, changing the flow configuration from co-current

to counter-current causes higher flux than the case when the ultrasound source faces the support layer.

A water flux regression model using $MgCl_2$ as a DS was developed using Minitab as shown in Eq. (4):

$$Y = 8.112 + 1.789X_1 + 0.113X_2 \\ - 0.835X_3 - 0.380X_1X_2 + 0.363X_1X_3 \\ + 0.060X_2X_3 + 0.072X_1X_2X_3 \qquad (4)$$

where $Y$ is the mean average water flux (response), $X_1$ is the CFV, $X_2$ is flow configuration, and $X_3$ is ultrasound orientation.

The $R$-squared value for the water flux model was determined to be 97.41%, which means 97.41% of the variability in the flux can be explained by the proposed model. To validate the regression model, the ANOVA table has been developed (data not shown). According to ANOVA table, the main effects due to velocity and ultrasound orientation are significant ($p$ value $< 0.05$). The two-parameter interactions between velocity and flow configuration and between velocity and ultrasound orientation are also significant. However, the two-parameter interaction between flow configuration and ultrasound configuration and the three-parameter interactions between velocity, flow configuration, and ultrasound orientation are insignificant.

ANOVA table also revealed that the model $F$-value of 43.06 and its associated $p$ value ($< 0.05$) demonstrate that the developed regression model is significant. Moreover, the model coefficients displayed in Table 7 agree with the ones provided by ANOVA. The Minitab generated residual plots for water flux using $MgCl_2$ as a DS are shown in Fig. 7. The normal probability plot demonstrates validity of the assumption that the residuals are normally distributed. This is confirmed by performing the Ryan–Joiner (RJ) (similar to Shapiro–Wilk) and Kolmogorov–Smirnov (KS) normality tests by having $p$ values of greater than 0.100 for the RJ test and greater than 0.150 for the KS test, both of them are greater than 0.05 which confirms the validity of the normality assumption.

Considering the case of $MgCl_2$ as a DS, and similar to the situation of NaCl DS, it can be concluded that the effect of increasing the CFV (from low to high level) provides a significant impact on the water flux. Changing the ultrasound location relative to the membrane surface (from SL to AL) causes a moderate effect on the flux (less than the effect of CFV). The change of flow direction from low to a high level (C to CC) causes a minor effect (statistically insignificant) on the water flux. The interaction effects were found to be similar to those observed in the NaCl test. However, it was noticed that the two-parameter interaction between velocity and flow configuration was significant in the $MgCl_2$ which was not the case with the NaCl situation.
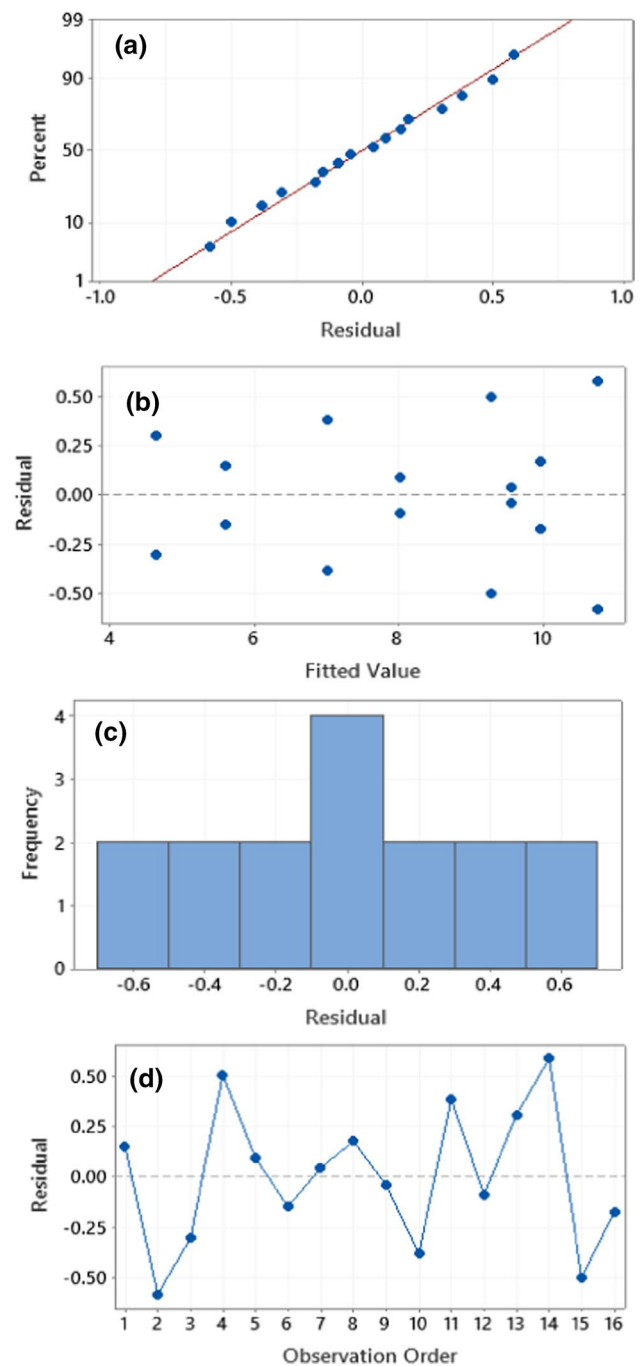


**Fig. 7** Residual plots for water flux ($L/m^2 \cdot h$) using $MgCl_2$ DS showing **a** normal probability plot, **b** residual versus fitted flux value, **c** frequency versus residual, and **d** residual versus observation order

## Comparison between NaCl and MgCl$_2$ draw solutions

In statistical analysis, the calculated values of the main effects and interaction effects provide information about the size and direction (positive or negative) regarding the relationship between the studied parameters and the required

response variable. The effects of CFV, flow configuration, and ultrasound orientation toward the membrane surface and their interactions explain the predicted change in the mean of the water flux when one or all of the selected parameters change their level from low to high or vice versa. To facilitate making a comparison between the main effects and interaction effects between the two DSs on the mean value of the water flux, the effect of each parameter and their interactions, along with the associated significance level are presented in Table 8. Moreover, the effect ratio between the NaCl and $MgCl_2$ was calculated for each term and is included in Table 8.

According to Table 8, significant effects of all parameters in the case of the NaCl DS were found higher than the effects obtained in the case of $MgCl_2$. The velocity term (changing from low to high) showed a significant positive effect of 6.141 on the mean of the water flux, while this value dropped to 3.577 in the case of the $MgCl_2$, which provides a velocity effect ratio of the NaCl relative to $MgCl_2$ of 1.72. The flow configuration in both cases (NaCl and $MgCl_2$) was not statistically significant; however, the effect ratio was about 2.08. The effect of ultrasound orientation toward the membrane surface (changing from SL to AL) for the NaCl case showed a higher positive effect ratio than the $MgCl_2$ of 2.17, where the effect of ultrasound in the NaCl case was 3.616 and decreased to 1.67 in the case of $MgCl_2$. It was observed that the ultrasound orientation in the case of NaCl DS showed a higher effect than velocity in the case of $MgCl_2$ DS. The effect of the two-parameter interaction between flow velocity (from low to high) flow configuration (from SL to AL) was insignificant in the NaCl case while found to be statistically significant in the case of $MgCl_2$. However, for the interaction effect between flow configuration and ultrasound orientation, an effect ratio of 2.76 was obtained. For both draw solutions, the two-parameter interaction between flow configuration and ultrasound orientation and the three-parameter interaction between velocity, flow configuration, and ultrasound orientation were found to be statistically insignificant. However, these interactions have

higher effect on water flux in the case of $MgCl_2$ compared to that of NaCl.

## Applicability of the developed relations to other data sets

In this work, it was attempted to verify the applicability of Eqs. (3) and (4) for prediction of other data sets. Equation (3) was developed for the experiments with NaCl DS while Eq. (4) was developed for the experiments with $MgCl_2$ DS. The question is: Could Eq. (3) be utilized to predict flux with the use of $MgCl_2$ DS and could Eq. (4) be utilized to predict flux with the use of NaCl DS? Predicted flux values using Eq. (3) for the tested cases with $MgCl_2$ DS and those using Eq. (4) for the tested cases with NaCl DS are plotted versus the actual flux values in Fig. 8.

Figure 8a shows that the majority of the predicted flux values using Eq. (3) for the experiments with $MgCl_2$ DS are clustered above the 1:1 line (i.e., the predicted values are higher than the actual ones), while Fig. 9b shows that the majority of the predicted flux values using Eq. (4) for the experiments with NaCl DS are clustered below the 1:1 line (i.e., the predicted values are lower than the actual ones). To measure the degree of correlation between the actual and
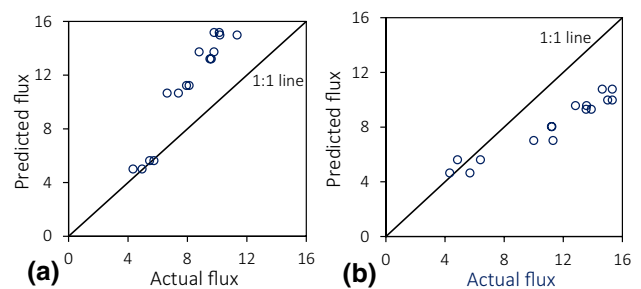


**Fig. 8** Predicted water flux ($L/m^2 \cdot h$) using **a** Eq. (3) for the experiments with $MgCl_2$ DS and **b** Eq. (4) for the experiments with NaCl DS

**Table 8** Comparison between the parameter effects of the NaCl and $MgCl_2$

| Term | Effect | | | Significant (Y)/ Insignificant (N) | |
|---|---|---|---|---|---|
| | NaCl | $MgCl_2$ | Effect ratio (NaCl/$MgCl_2$) | NaCl | $MgCl_2$ |
| Velocity | **6.141** | **3.577** | 1.72 | Y | Y |
| Flow Conf. | 0.471 | 0.226 | 2.08 | N | N |
| US Orien. | **−3.616** | **−1.670** | 2.17 | Y | Y |
| Velocity × Flow Conf. | −0.119 | **−0.759** | 0.16 | N | Y |
| Velocity × US Orien. | **2.009** | **0.727** | 2.76 | Y | Y |
| Flow Conf. × US Orien. | 0.099 | 0.12 | 0.83 | N | N |
| Velocity × Flow Conf. × US Orien. | 0.069 | 0.144 | 0.48 | N | N |

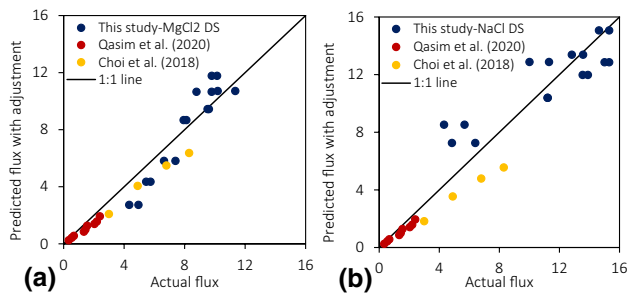Bold values indivcated by the 95% confidence interval

**Fig. 9** Predicted water flux ($L/m^2 \cdot h$) with adjusted **a** Eq. (3) and **b** Eq. (4)

predicted flux, the Spearman's correlation coefficient ($r_s$) given by Eq. (5) is used.

$$r_s = 1 - \frac{6 \sum_1^n \left( J_{w\text{-actual}} - J_{w\text{-predicted}} \right)^2}{n\left(n^2 - 1\right)} \qquad (5)$$

where $J_{w\text{-actual}}$ is the actual flux, $J_{w\text{-predicted}}$ is the predicted flux and $n$ is the number of data points. For both data sets, the $r_s$ value is 0.7, indicating a medium to strong correlation. However, the predictions could be improved if normalization to the baseline conditions is considered as shown in Fig. 9. The predicted flux after adjustment (Fig. 9) was obtained by multiplying the predicted flux values using Eqs. (3) or (4) by the ratio of the baseline flux of the examined case relative to the baseline flux of the case that belongs to the pool of data utilized to develop the equation. For example, Eq. (3) predicts a flux value of 10.66 $L/m^2 \cdot h$ with MgCl$_2$ DS under the conditions of low CFV, co-current flow, and the ultrasound facing the membrane active layer, while the actual flux value for this case is 6.64 $L/m^2 \cdot h$ (Table 6). Given that the baseline flux for the case is 4.33 $L/m^2 \cdot h$ and the baseline flux for the same case with NaCl DS is 7.95 $L/m^2 \cdot h$ (Table 2), the predicted flux after adjustment is $10.66 \times (4.34/7.95) = 5.82$ $L/m^2 \cdot h$. With the made adjustment, the flux is better predicted, and the data of this study fluctuate around the 1:1 line rather than being clustered on one side of the line. The degree of correlation ($r_s$) between the actual and predicted flux with MgCl$_2$ DS of this study based on Eq. (3) increased from 0.7 to 0.96 after adjustment. Similarly, the value of $r_s$ increased from 0.7 to 0.91 upon adjustment of Eq. (4) to predict flux with NaCl DS in this study. This indicates a very strong correlation between the actual and predicted flux after adjustment.

For the data of this study, three cases in Fig. 9a have predicted flux values that exceed the actual flux values by more than 10%, while six cases have predicted values that are lower by more than 10%. Cases with over-predicted flux values by Eq. (3) are those that have been conducted at high CFV with counter-current flow, while those with under-predicted flux values have been conducted at low CFV.

However, the situation is reversed with the use of Eq. (4) (i.e., the cases of this study that are significantly under-predicted by Eq. (3) are significantly over-predicted by Eq. (4) and vice versa).

Application of Eqs. (3) and (4) could be extended to data sets reported by others assuming that the CFV used by others is close to the values examined in this study and that other experimental conditions such as applied frequency and ultrasound operation mode are the same. The data of Qasim et al. (2020) fulfill such requirements and some of the data points reported by Choi et al. (2018) could potentially be used for such purpose. Other studies that have been conducted on ultrasound-assisted FO cannot be utilized to validate Eqs. (3) and (4) because either they applied intermittent (not continuous) ultrasound mode (Chanukya and Rastogi 2017; Nguyen et al. 2015), the applied ultrasound frequency significantly deviates from the one used in this study (Choi et al. 213; Heikkinen et al. 2017), or they did not report the applied ultrasound frequency (Kim et al. 2012).

Qasim et al. (2020) investigated the effect of ultrasound on the performance of the FO process with MgSO$_4$ and CuSO$_4$ draw solutions. They used a CTA FO flat sheet membrane in a co-current flow arrangement. Their experimental setup is identical to one used in this study in terms of the testing cell dimensions and the ultrasound device type and arrangement. They utilized simulated brackish water (5000 mg/L NaCl) and seawater (40,000 mg/L NaCl) as a feed solution. The testing was conducted at a CFV of 1.1 cm/s with continuous ultrasound facing the membrane support layer at a frequency of 40 kHz. CuSO$_4$ DS at three concentrations (0.5, 0.75, and 1 mol/L) was tested for desalination of brackish water, while MgSO$_4$ DS at three concentrations (1.5, 1.75, and 2.0 M) was tested for desalination of both brackish water and seawater. Given that the authors applied one testing arrangement in terms of CFV, flow configuration and ultrasound orientation, the predicted flux for all their tested cases using Eqs. (3) and (4) without adjustment would be 13.2 and 9.6 $L/m^2 \cdot h$, respectively. These values significantly deviate from their reported values of 2.04–2.4 $L/m^2 \cdot h$ with MgSO$_4$ DS and 0.34–1.56 $L/m^2 \cdot h$ with CuSO$_4$ DS. However, after consideration of flux under baseline conditions, the predicted flux values closely match the actual flux values as shown in Fig. 9, with $r_s$ of 0.98 for both.

Choi et al. (2018) studied the effect of ultrasound on FO flux enhancement using a CTA membrane and a counter-current flow configuration. NaCl solution of 0.5 M was used as the system feed, while 1–4 M NaCl solution was used as a draw solution. Testing was conducted at a CFV of 4.4 cm/s. The authors used an ultrasound transducer with a 5.0-cm-diameter tip that was placed 1.0 cm facing the membrane support layer. They tested the effect of different ultrasound output power (10, 30, 50, and 70 W) at different frequencies (25, 45, and 72 kHz). Of the data reported by Choi et al.

(2018), the most suitable ones that could be used to validate Eqs. (3) and (4) are those produced with an ultrasound frequency of 45 kHz at an output power of 10 W, which corresponds to an ultrasound intensity of 0.47 W/cm$^2$ at the membrane surface. Tested cases with an output power other than 10 W result in higher ultrasound intensities and thus deviate more from the ultrasound intensity employed in this study (0.09 W/cm$^2$). Since the authors applied one testing arrangement in terms of CFV, flow configuration and ultrasound orientation, the predicted flux values for their tested cases at a frequency of 45 kHz and an output power of 10 W would be 13.7 and 9.3 L/m$^2$·h based on the unadjusted Eqs. (3) and (4). Compared to their reported flux values (3.0–8.3 L/m$^2$·h), the predicted values have an average absolute deviation of 176 and 87% when using Eq. (3) and (4), respectively. However, after adjustment of Eqs. (3) and (4), the average absolute deviation drops to 22.6 and 32.5%, respectively. Nonetheless, the degree of correlation ($r_s$) between the actual and predicted flux values based on Eq. (3) is 0.296, while that based on Eq. (4) is −0.486. These values do not indicate a strong correlation between the two variables.

As shown in Fig. 9, the actual flux of Choi et al. is lower than the predicted one for all considered points. This could be attributed to the higher CFV they used (4.4 cm/s) as compared to the upper value used in developing Eqs. (3) and (4). It could also be due to the higher ultrasound intensity employed in their study. Both factors (CFV and ultrasound intensity) are expected to positively cause an enhancement of flux. Thus, the use of Eq. (3) and (4) to predict flux for cases with crossflow velocities or for applied ultrasound intensities that differ from the ones used in this study may not be valid.

## Conclusions

With the use of NaCl as a draw solution, the effect of changing the flow velocity (from low to high) caused a significant increase in water flux. Changing the flow configuration from co-current to counter current caused a slight water flux enhancement, which was found to be statistically insignificant. Changing the ultrasound orientation from the support to the active layer caused a significant increase in water flux. No significant interaction between the flow velocity and flow configuration and between the flow configuration and the ultrasound orientation that significantly affected the water flux. However, the interaction effect between flow velocity and ultrasound orientation caused a significant effect on the membrane water flux.

With the use of MgCl$_2$ as a draw solution, changing the flow velocity from low to high caused a significant water flux enhancement. Changing the ultrasound orientation from the support to the active layer caused a moderate flux

enhancement. The effect of flow configuration was not statistically significant. However, the two-way interaction of the flow configuration by the ultrasound orientation was found to have a marginal effect on water flux. A marginal effect of the interaction between the flow velocity and the ultrasound orientation was also noticed.

The effect of flow velocity and ultrasound orientation on flux was 1.72 and 2.08 times higher with the use of NaCl as compared to that when MgCl$_2$ was used. Moreover, the interaction effect of flow velocity by the ultrasound orientation with NaCl was 2.8 times higher than the one found with the use of MgCl$_2$.

The factorial model equations developed in this work can be used to adequately predict flux in ultrasound-assisted FO systems at relatively similar conditions after adjustment of the model for the baseline conditions of the evaluated cases.

## Declarations

**Conflict of interest** The authors declare no conflict of interest. This paper represents the opinions of the authors and does not mean to represent the position or opinions of the American University of Sharjah. The authors also declare that they have no known competing financial interests or personal relationships that could influence the work reported in this paper.

## References

Achilli A, Cath TY, Childress AE (2010) Selection of inorganic-based draw solutions for forward osmosis applications. J Mem Sci 364(1):233–241. https://doi.org/10.1016/j.memsci.2010.08.010
Aktij SA, Taghipour A, Rahimpour A, Mollahosseini A, Tiraferri A (2020) A critical review on ultrasonic-assisted fouling control and cleaning of fouled membranes. Ultrasonics 108:106228. https://doi.org/10.1016/j.ultras.2020.106228
Al-Sakaji BAK, Al-Asheh S, Maraqa MA (2022a) A review on the development of an integer system coupling forward osmosis membrane and ultrasound waves for water desalination processes. Polymers 14:2710. https://doi.org/10.3390/polym14132710
Al-Sakaji BAK, Al-Asheh S, Maraqa MA (2022b) Effects of operating conditions on the performance of forward osmosis with ultrasound

for seawater desalination. Water 14:2092. https://doi.org/10.3390/w14132092

Cath T, Childress A, Elimelech M (2006) Forward osmosis: principles, applications, and recent developments. J Mem Sci 281(1–2):70–87. https://doi.org/10.1016/j.memsci.2006.05.048

Cath TY, Elimelech M, McCutcheon JR, McGinnis RL, Achilli A, Anastasio D, Brady AR, Childress AE, Farr IV, Hancock NT, Lampi J, Nghiem LD, Xie M, Yip NY (2013) Standard methodology for evaluating membrane performance in osmotically driven membrane processes. Desalination 312:31–38. https://doi.org/10.1016/j.desal.2012.07.005

Chanukya BS, Rastogi NK (2017) Ultrasound assisted forward osmosis concentration of fruit juice and natural colorant. Ultrason Sonochem 34:426–435. https://doi.org/10.1016/j.ultsonch.2016.06.020

Choi YJ, Kim SH, Jeong S, Hwang TM (2014) Application of ultrasound to mitigate calcium sulfate scaling and colloidal fouling. Desalination 336:153–159. https://doi.org/10.1016/j.desal.2013.10.011

Choi Y, Hwang TM, Jeong S, Lee S (2018) The use of ultrasound to reduce internal concentration polarization in forward osmosis. Ultrason Sonochem 41:475–483. https://doi.org/10.1016/j.ultsonch.2017.10.005

Kah PL, Tom CA, Davide M (2011) A review of reverse osmosis membrane materials for desalination—development to date and future potential. J Mem Sci 370:1–22. https://doi.org/10.1016/j.memsci.2010.12.036

Kim H, Lee Y, Elimelech M, Adout A, Kim YC (2012) Experimental study of ultrasonic effects on flux enhancement in forward osmosis process. The Electrochemical Society, Meeting Abstract MA2012-01 90. 2012. https://iopscience.iop.org/article/10.1149/MA2012-01/4/90/pdf. Accessed 1 May 2022

Heikkinen J, Kyllönen H, Järvelä E, Grönroos A, Tang CY (2017) Ultrasound-assisted forward osmosis for mitigating internal concentration polarization. J Mem Sci 528:147–154. https://doi.org/10.1016/j.memsci.2017.01.035

Lee WJ, Ng ZC, Hubadillah SK, Goh PS, Lau WJ, Othman MHD, Ismail AF, Hilal N (2020) Fouling mitigation in forward osmosis and membrane distillation for desalination. Desalination 480:114338. https://doi.org/10.1016/j.desal.2020.114338

Mason RL, Gunst RF, Hess JL (2003) Statistical design and analysis of experiments: with applications to engineering and science. John Wiley & Sons, New York

Mi B, Elimelech M (2008) Chemical and physical aspects of organic fouling of forward osmosis membranes. J Mem Sci 320:292–302

Minitab software: data analysis, statistical & process improvement tools. https://www.minitab.com/en-us/. Accessed 20 Mar 2021

Montgomery DC (2013) Design and analysis of experiments, 8th edn. Wiley, Hoboken

Nguyen NC, Nguyen HT, Chen SS, Nguyen NT, Li CW (2015) Application of forward osmosis (FO) under ultrasonication on sludge thickening of waste activated sludge. Water Sci Technol 72(8):1301–1307. https://doi.org/10.2166/wst.2015.341

Nollet JA (1764) Lecons de Physique Experimentale. Hippolyte-Louis Guerin and Louis-Francios Delatour, Paris

Phuntsho S, Hong S, Elimelech M, Shon HK (2013) Forward osmosis desalination of brackish groundwater: Meeting water quality requirements for fertigation by integrating nanofiltration. J Mem Sci 436:1–15. https://doi.org/10.1016/j.memsci.2013.02.022

Qasim M, Darwish NA, Sarp S, Hilal N (2015) Water desalination by forward (direct) osmosis phenomenon: a comprehensive review. Desalination 374:47–69. https://doi.org/10.1016/j.desal.2015.07.016

Qasim M, Mohammed F, Aidan A, Darwish NA (2017) Forward osmosis desalination using ferric sulfate draw solute. Desalination 423:12–20. https://doi.org/10.1016/j.desal.2017.08.019

Qasim M, Darwish NN, Mhiyo S, Darwish NA, Hilal N (2018) The use of ultrasound to mitigate membrane fouling in desalination and water treatment. Desalination 443:143–164. https://doi.org/10.1016/j.desal.2018.04.007

Qasim M, Khudhur FW, Aidan A, Darwish NA (2020) Ultrasound-assisted forward osmosis desalination using inorganic draw solutes. Ultrason Sonochem 61:104810. https://doi.org/10.1016/j.ultsonch.2019.104810

Robert LM, Menachem E (2007) Energy requirements of ammonia–carbon dioxide forward osmosis desalination. Desalination 207:370–382. https://doi.org/10.1016/j.desal.2006.08.012

Seltman HJ (2018) Experimental design and analysis. Carnegie Mellon University, Pittsburgh, PA, p 428

Suwaileh W, Pathak N, Shon H, Hilal N (2020) Forward osmosis membranes and processes: a comprehensive review of research trends and future outlook. Desalination 485:114455. https://doi.org/10.1016/j.desal.2020.114455

Tai-Shung C, Sui Z, Kai YW, Jincai S, Ming ML (2012) Forward osmosis processes: yesterday, today and tomorrow. Desalination 287:78–81. https://doi.org/10.1016/j.desal.2010.12.019

Tzahi Y, Cath AE, Childress ME (2006) Forward osmosis: principles, applications, and recent developments. J Mem Sci 281:70–87. https://doi.org/10.1016/j.memsci.2006.05.048

Xu Y, Peng X, Tang CY, Fu QS, Nie S (2010) Effect of draw solution concentration and operating conditions on forward osmosis and pressure retarded osmosis performance in a spiral wound module. J Mem Sci 348(1–2):298–309. https://doi.org/10.1016/j.memsci.2009.11.013